Channelrhodopsin-1: A Light-Gated Proton Channel in Green Algae

Georg Nagel,[1]* Doris Ollig,[1] Markus Fuhrmann,[2] Suneel Kateriya,[2] Anna Maria Musti,[3] Ernst Bamberg,[1] Peter Hegemann[2]

Phototaxis and photophobic responses of green algae are mediated by rhodopsins with microbial-type chromophores. We report a complementary DNA sequence in the green alga *Chlamydomonas reinhardtii* that encodes a microbial opsin-related protein, which we term Channelopsin-1. The hydrophobic core region of the protein shows homology to the light-activated proton pump bacteriorhodopsin. Expression of Channelopsin-1, or only the hydrophobic core, in *Xenopus laevis* oocytes in the presence of all-*trans* retinal produces a light-gated conductance that shows characteristics of a channel selectively permeable for protons. We suggest that Channelrhodopsins are involved in phototaxis of green algae.

The earliest detectable rhodopsin-mediated responses in phototactic green algae are electrical currents within the eye spot. These currents are carried by Ca^{2+} and H^+ (*1*, *2*). In *Chlamydomonas reinhardtii* or *Haematococcus pluvialis*, photoreceptor currents occur with a delay of <30 μs after flash stimulation (*3*, *4*), suggesting an intimate link between photoreceptor and electrical conductance. The two dominant retinal-binding proteins in the eye spot, Cop1 and Cop2, are not the photoreceptors that mediate photomovement responses (*5*). Searching a *C. reinhardtii* EST (expressed sequence tag) database (*6*) revealed overlapping cDNA sequences that encode a 76.4-kD opsin-related protein. We have named this protein Channelopsin-1 (Chop1). The core region (amino acid residues 76 to 309 out of 712 total) comprises seven hypothetical transmembrane segments with sequence similarity (15 to 20%) to the archaeal sensory rhodopsins (SRs), the ion transporters bacteriorhodopsin (BR) and halorhodopsin (HR), and rhodopsin from *Neurospora* (nop1) (*7*). Although the overall sequence homology is low, several amino acids are conserved that define the retinal-binding site and the H^+-transporting network in BR (*8*, *9*) (Fig. 1 and Supporting Online Material). The consensus motif LDxxxKxxW (*10*) suggests that K296 is the retinal-binding amino acid. Thirteen of the 22 amino acids that are in contact with the retinal in BR are identical (9 amino acids) or conservatively exchanged (4 amino acids) in Chop1. The conserved residues are close to the protonated Schiff-base site in the archaeal rhodopsins.

We expressed cRNA encoding Chop1 in oocytes of *Xenopus laevis*, in the presence of all-*trans* retinal, to study ion transport under voltage-clamp conditions, as demonstrated for BR and sensory rhodopsin II (*11*–*13*). Illumination by green light, but not red light, induced inward currents in *Chop1* RNA–injected oocytes at a membrane potential of –100 mV (Fig. 2A). Similar results were obtained with truncated *Chop1* RNAs encoding amino acids 1 to 346 or 1 to 517. At an external pH (pH_o) of 7.5, the inward current induced by green light reversed at a voltage near –15 mV (Fig. 2B) with clearly visible outward photocurrents at positive membrane potentials. The dependence of photocurrent direction on the applied potential suggests that the reconstituted Channelrhodopsin-1 (ChR1) mediates a light-induced passive ion conductance. A reversal potential of –15 mV is close to the Nernst potential for Cl^- [–20 mV, as deduced by expressing CFTR (cystic fibrosis transmembrane conductance regulator) Cl^- channels in oocytes (*14*)] or H^+ [–12 mV, at an intracellular pH (pH_i) of 7.3, as measured with microelectrodes by us and others (*15*)], but far from Nernst potentials for Na^+, K^+, or Ca^{2+}.

To investigate the ionic specificity of the light-induced permeability, we systematically changed the composition of the bath solution. Lowering the pH_o to 6.0 increased inward photocurrents and shifted the reversal potential to >+40 mV (Fig. 3, A and B). Replacing Cl^- by aspartate (pH_o = 6) had no discernible effect on the photocurrent amplitude or its current-voltage (*I-V*) relation (Fig. 3, A and B), thus excluding Cl^- as the conducted ion. Similarly, Na^+ and Ca^{2+} were excluded: Photocurrents were not changed either by replacing Na^+ by *N*-methyl-D-glucamine (NMG) or by replacing Ca^{2+} with Mg^{2+} (Fig. 3, A and B). However, increasing the H^+ concentration of the bath solution, $[H^+]_o$, to 10 μM (pH_o = 5) enhanced the light-induced inward currents, and changing

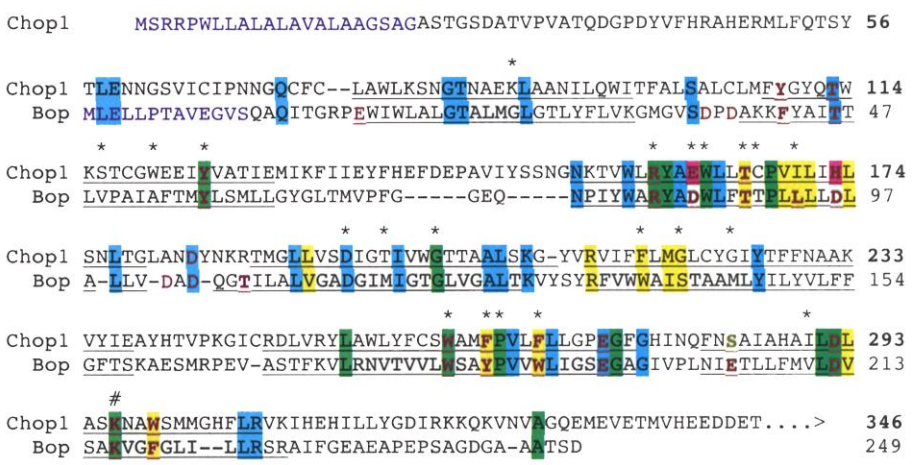

Fig. 1. Comparison of the truncated Chop1 (GenBank accession no. AF385748) sequence (*10*), Chop1-346 (encoding amino acids 1 to 346), with bacterioopsin (Bop) from *Halobacterium salinarum*. Amino acids that are known from the bacteriorhodopsin (BR) structure to interact directly with the retinal (*8*, *9*) are indicated with an asterisk (*). Amino acids that are identical in most microbial opsins are highlighted in green; those that are functionally homologous in microbial opsin sequences are in yellow; and those that are identical in Chop1, BR, and only some other microbial opsins are in blue. Amino acids that contribute to the H^+-conducting network in BR (*8*, *9*) are shown in red. Residues that are part of the transmembrane H^+-network are in bold type. The key substitutions, D^{85} and D^{96} in BR to E^{162} and H^{173} in Chop1, are shown in red. Underlined amino acids indicate identified or hypothetical transmembrane helices. Amino acids labeled in blue are leader sequences. The numbering of bacterioopsin begins after the leader sequence for historical reasons. The hypothetical retinal-binding Lys is labeled with "#". For further details, see supporting online material.

[1]Max-Planck-Institut für Biophysik, Kennedyallee 70, 60596 Frankfurt am Main, Germany. [2]Institut für Biochemie, Universität Regensburg, Universitätsstrasse 31, 93040 Regensburg, Germany. [3]Dipartimento Farmaco-Biologico Università della Calabria, 87036 Rende, Italy.

*To whom correspondence should be addressed. E-mail: nagel@mpibp-frankfurt.mpg.de

$[H^+]_o$ to 100 μM (pH_o = 4) further increased the photocurrents (Fig. 3, A to C). Figure 3C demonstrates the magnitude of light-induced H^+ currents at pH_o = 4 in an oocyte where light-induced H^+ conductance exceeds the background conductance of the oocyte by more than fivefold. Lowering pH_o shifts the reversal potential of the photocurrent to more positive values (Fig. 3B). Taken together, these results indicate that the photocurrent is carried by protons.

The reversal potential of the photocurrent should be shifted to more negative potentials by increasing the cytosolic $[H^+]$. At pH_o = 7.4, a concentration of 40 mM Na-butyrate, which corresponds to 100 μM undissociated, membrane-permeable butyric acid, has been reported to increase the cytosolic $[H^+]$ of an oocyte from 50 nM (pH_i = 7.3) to 160 nM (pH_i = 6.8) (*15*). We confirmed by pH measurements with ion-selective microelectrodes at pH_o = 7.4 that 40 mM butyrate caused a 0.5-unit decrease in pH_i. At pH_o = 7.4, 100 μM butyric acid caused a shift of the photocurrent reversal potential from –5 ± 2 mV to –33 ± 2 mV (n = 5) (Fig. 3D). Photocurrents were measured at four pH_o values—7.4, 7.0, 6.6, and 6.2—with the undissociated butyric acid concentration of 100 μM to maintain the pH_i at ~6.8 (*15*). The direction of photocurrent reversed at a different potential for each pH_o (Fig. 3D). The dependence of

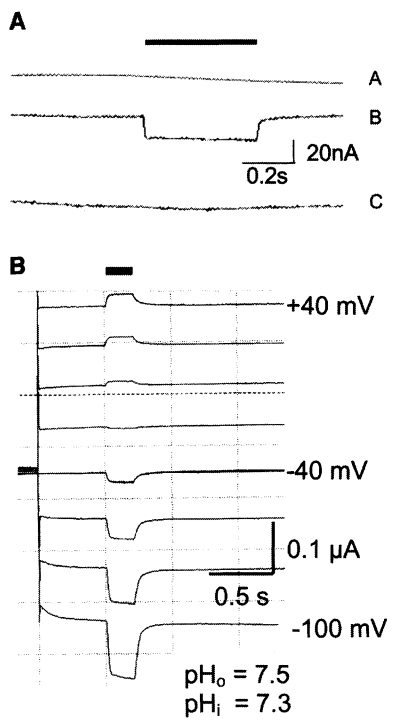

Fig. 2. Light and voltage dependence of photocurrents at pH = 7.5. (**A**) Photocurrents recorded during illumination of oocytes with green or red light (500 ± 25 nm or 700 ± 25 nm, respectively; 10^{22} photons m^{-2} s^{-1}). Membrane potential (V) = –100 mV; the light pulse is indicated by a bar. Bath solution: 96 mM NaCl, 5 mM KCl, 2 mM $CaCl_2$, 1 mM $MgCl_2$, 5 mM MOPS (pH = 7.5). Trace A: A noninjected oocyte, green light. Trace B: A Chop1 oocyte, green light. Trace C: The same Chop1 oocyte as in trace B, irradiated with red light. (**B**) Current responses of a Chop1 oocyte to voltage steps from –100 mV to +40 mV (in 20-mV steps; holding potential V_h = –40 mV), followed by green light pulses of 200-ms duration. Bath solution: 96 mM NaCl, 5 mM KCl, 2 mM $CaCl_2$, 1 mM $MgCl_2$, 5 mM MOPS (pH = 7.5).

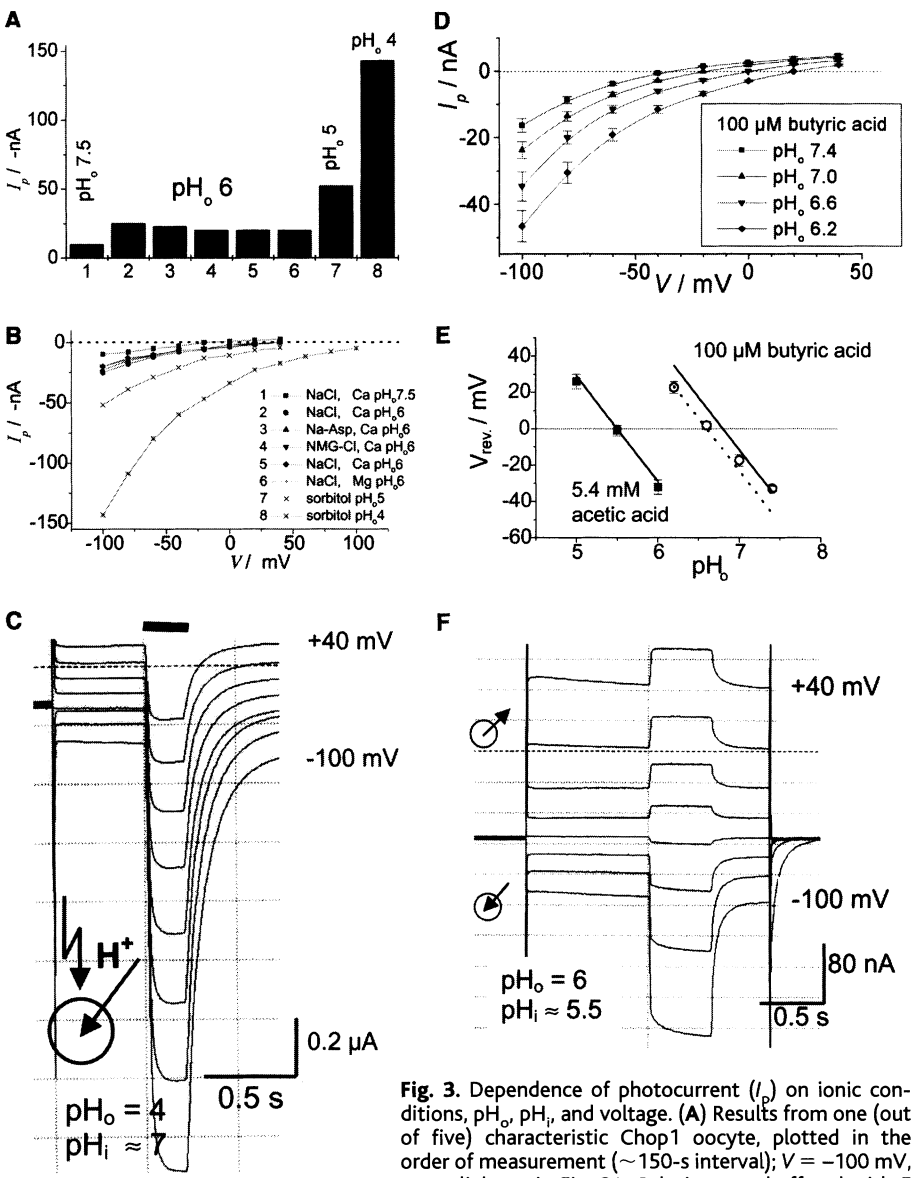

Fig. 3. Dependence of photocurrent (I_p) on ionic conditions, pH_o, pH_i, and voltage. (**A**) Results from one (out of five) characteristic Chop1 oocyte, plotted in the order of measurement (~150-s interval); V = –100 mV, green light as in Fig. 2A. Solutions are buffered with 5 mM MOPS (pH = 7.5), MES (pH = 6), or citrate (pH = 5 and 4). Concentration (in mM): bar 1: 100 NaCl, 2 $CaCl_2$ (pH = 7.5); bar 2: 100 NaCl, 2 $CaCl_2$ (pH = 6.0) (reference condition); bar 3: 100 Na-aspartate, 2 $CaCl_2$ (pH = 6.0); bar 4: 100 NMG-Cl, 2 $CaCl_2$ (pH = 6.0); bar 5: same as bar 2; bar 6: 100 NaCl, 2 EGTA, 2 $MgCl_2$ (pH = 6.0); bar 7: 200 sorbitol, 5 EGTA (pH = 5.0); bar 8: 200 sorbitol, 5 EGTA (pH = 4.0). (**B**) Voltage dependence of photocurrents (I_p) from (A). Concentrations as in (A). (**C**) Current responses to voltage jumps from –100 to +40 mV (in 20-mV steps, V_h = –40 mV), followed by green light pulses of 200-ms duration. Bath solution: 200 mM sorbitol, 5 mM citrate (pH = 4.0) with NMG (same oocyte as in Fig. 2B). (**D**) Voltage dependence of photocurrent (I_p) in different bath solutions, containing 100 μM undissociated butyric acid: (■) 60 mM NaCl + 40 mM Na-butyrate (pH = 7.4); (▲) 84 mM NaCl + 16 mM Na-butyrate (pH = 7.0); (▼) 93.6 mM NaCl + 6.4 mM Na-butyrate (pH = 6.6); (◆) 97.4 mM NaCl + 2.6 mM Na-butyrate (pH = 6.2) (n = 5). (**E**) (○) pH_o dependence of reversal potentials, derived from (D). The lines show the theoretical relation for a proton-selective conductance (–58 mV/pH) at a constant pH_i of 6.6 (dotted) or 6.8 (solid). (■) pH_o dependence of reversal potentials, derived from experiments (n = 6) with 5.4 mM undissociated acetic acid, as demonstrated in (F). The line shows the theoretical relation for a constant pH_i of 5.5 and –58 mV/pH. (**F**) Current responses to voltage steps from V = –100 mV to +40 mV, followed by green light pulses. Bath solution: 100 mM Na-acetate, 5 mM MES (pH = 6.0) with NaOH.

reversal potential (V_{rev}) on pH_o is shown in Fig. 3E (open circles). The V_{rev} of –33 ± 2 mV at pH_o = 7.4 and pH_i = 6.8 (*15*) is in close agreement with the H^+ V_{rev} of –35 mV at ΔpH = 0.6. This close fit shows that the light-activated currents are passive. In addition, the dependence of photocurrent V_{rev} on pH_o indicates a high selectivity for protons. A small change of pH_i with changing pH_o, as reported previously for oocytes (*15*), can explain the deviation from the ideal slope of –58 mV/pH unit. Indeed, a shift of pH_i from 6.8 to 6.6 (as shown by the two lines with ideal slope in Fig. 4C) would bring the observed dependence in accordance with theoretical expectation for a photoconductance that is selectively permeable for H^+. When a high concentration (5.4 mM) of undissociated acetic acid (pH_o = 5 to 6) was administered, large outward photocurrents at positive potentials (Fig. 3F) and an ideally pH_o-dependent V_{rev} with a slope of –58 mV/pH unit were observed (Fig. 3E, filled circles). The V_{rev} observed in these experiments suggests that application of 5.4 mM acetic acid lowers the pH_i to ~5.5 (Fig. 3E). We confirmed this value using microelectrodes to measure the pH_i of oocytes in the presence of 5.4 mM acetic acid. Thus, the observed dependence of V_{rev} on pH_o implies that the ChR1-mediated light-sensitive conductance is passive and highly selective for protons.

The dependence of the direction of proton transport on the electrochemical potential for H^+ is compatible with either facilitated diffusion of a stoichiometric number of protons during each ChR1 photocycle or a light-gated proton channel in which an intermediate of the ChR1 photocycle allows permeation of many H^+ ions. However, further analysis supported the model of a light-gated channel. The photocurrent decays with two time constants after illumination, similar to bacteriorhodopsin (*16*) (Fig. 4A). These time constants are strongly temperature sensitive, indicating an activation energy for the photocycle of ~60 kJ/mol. The temperature sensitivity of the photocurrent amplitude is much smaller, ~20 kJ/mol (Fig. 4, A and B). This suggests that intermediates of the photocycle serve as the proton-conducting channel. The maximal ChR1 photocurrent exceeds maximal BR photocurrents, providing an additional argument against a stoichiometric coupling of photocycle and proton transport. Large photocurrents of a strictly coupled system would require either a photocycle that is faster than that of BR, which is incompatible with the observed slow decay time constants, or a high expression level (~100-fold greater than that of BR), which is unlikely. If we assume that the level of ChR1 expression in oocytes is similar to that of BR [~2×10^9 molecules per oocyte (*11*)], then we can calculate the electrical current contribution of a single ChR1 molecule. At pH_o = 4 and –100 mV, we measured a light-induced inward current of ~1.4 μA, i.e., ~4000 protons/s or 0.7 fA per molecule, which is much too small for single-channel resolution.

The wavelength dependence of the inward photocurrent was determined at pH_o = 5.5 and –40 mV (Fig. 4C). The maximum wavelength of ~500 nm closely resembles that observed in the action spectra for photoreceptor currents (*1*), phototaxis (*17*), and photoshock responses (*18*) of intact *C. reinhardtii* cells. The pH_o-dependent photocurrent, I_{P2}, recorded from intact *C. reinhardtii* cells (*2*) was found to dominate the stationary current in continuous light at low pH_o (*2*). We speculate that I_{P2} might be carried by ChR1.

During the BR photocycle, a proton is transferred from the Schiff base to Asp^{85} (corresponding to Glu^{162} in Chop1) and released to the surface by way of Arg^{82}, Glu^{194}, and Glu^{204}. The corresponding residues in Chop1 are Arg^{161}, Glu^{274}, and Ser^{284}. The key amino acid for the reprotonation of the retinal Schiff base in BR is Asp^{96} (*8*, *19*). The corresponding amino acid in Chop1 is His^{173} (Fig. 1), which we exchanged with three different amino acids: Asp, Arg, or Tyr. The substitution His^{173} → Asp (H173D) resulted in a complete loss of light-gated conductance, whereas H173R or H173Y were still functional (Fig. 4D). These results indicate that His^{173} does not function as a proton donor of a deprotonated Schiff base. Therefore, we suggest that in ChR1 the retinal Schiff base is not deprotonated during the photocycle. This claim is corroborated by the observation that blue light, which is absorbed by deprotonated retinylidene, did not quench the stationary currents (*20*). It is conceivable that isomerization of retinal or a conformational change, tightly coupled to isomerization, gates the ChR1 proton channel.

In conclusion, ChR1 is an ion channel that opens in response to absorption of light, i.e., a combined photoreceptor and ion channel. It is not unlikely that such directly light-sensitive ion channels are widely distributed in other phototactic microalgae, as well as in gametes and zoospores of macroalgae, or even in fungi (e.g., nop1) (*7*). Moreover, the ability of ChR1 to mediate a large light-switched H^+ conductance in oocytes holds promise for the use of ChR1 as a tool for measuring and/or manipulating electrical and proton gradients across cell membranes, simply by illumination.

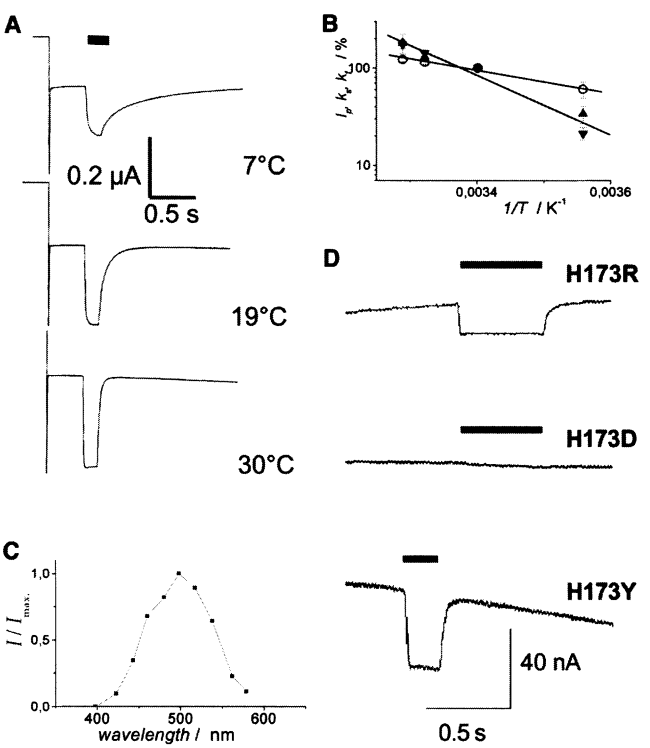

Fig. 4. Dependence of photocurrent on temperature, wavelength, and amino acid at position 173. (**A**) Current at –100 mV (voltage steps from –40 mV) and pH_o = 4 at 7°, 19°, and 30°C (same oocyte). Decay of photocurrent was fitted with a biexponential function at all three temperatures: 7°C: τ_f = 115 ms, τ_s = 810 ms; 19°C: τ_f = 35 ms, τ_s = 150 ms; 30°C: τ_f = 19 ms, τ_s = 49 ms. (**B**) Arrhenius plot of inverse time constants [(▼) k_s, (▲) k_f] and photocurrent [(○) I_p] from four experiments. Lines indicate an activation energy of 22 kJ/mol for I_p and 60 kJ/mol for k_s and k_f. (**C**) Wavelength dependence of the light-induced inward current at pH_o = 5.5 and –40 mV. The photocurrents were corrected for equal photon flux. (**D**) Photocurrents of mutants Chop1-H173R, Chop1-H173D, and Chop1-H173Y at –80 mV, pH_o = 5.

References and Notes

1. H. Harz, P. Hegemann, *Nature* **351**, 489 (1991).
2. S. Ehlenbeck, D. Gradmann, F.-J. Braun, P. Hegemann, *Biophys. J.* **82**, 740 (2001).
3. O. A. Sineshchekov, F. F. Litvin, L. Keszthelyi, *Biophys. J.* **57**, 33 (1990).
4. E. M. Holland, F. J. Braun, C. Nonnengässer, H. Harz, P. Hegemann, *Biophys. J.* **70**, 924 (1996).
5. M. Fuhrmann, A. Stahlberg, S. Rank, E. Govorunova, P. Hegemann, *J. Cell Sci.* **114**, 3857 (2001).
6. E. Asamizu *et al.*, *DNA Res.* **7**, 305 (2000).

7. J. Bieszke *et al.*, *Proc. Natl. Acad. Sci. U.S.A.* **96**, 8034 (1999).
8. R. Henderson *et al.*, *J. Mol. Biol.* **213**, 899 (1990).
9. J. K. Lanyi, H. Luecke, *Curr. Opin. Struct. Biol.* **11**, 415 (2001).
10. Single-letter abbreviations for the amino acid residues are as follows: A, Ala; C, Cys; D, Asp; E, Glu; F, Phe; G, Gly; H, His; I, Ile; K, Lys; L, Leu; M, Met; N, Asn; P, Pro; Q, Gln; R, Arg; S, Ser; T, Thr; V, Val; W, Trp; and Y, Tyr. x, any amino acid.
11. G. Nagel, B. Möckel, G. Büldt, E. Bamberg, *FEBS Lett.* **377**, 263 (1995).
12. G. Nagel, B. Kelety, B. Möckel, G. Büldt, E. Bamberg, *Biophys. J.* **74**, 403 (1998).
13. G. Schmies, M. Engelhard, P. G. Wood, G. Nagel, E. Bamberg, *Proc. Natl. Acad. Sci. U.S.A.* **98**, 1555 (2001).
14. G. Nagel, T. Szellas, J. R. Riordan, T. Friedrich, K. Hartung, *EMBO Rep.* **2**, 249 (2001).
15. A. K. Stewart, M. N. Chernova, Y. Z. Kunes, S. L. Alper, *Am. J. Physiol. Cell Physiol.* **281**, C1344 (2001).
16. S. Geibel *et al.*, *Biophys. J.* **81**, 2059 (2001).
17. K. W. Foster *et al.*, *Nature* **311**, 756 (1984).
18. R. Uhl, P. Hegemann, *Biophys. J.* **58**, 1295 (1990).
19. H. J. Butt, K. Fendler, E. Bamberg, J. Tittor, D. Oesterhelt, *EMBO J.* **8**, 1657 (1989).
20. G. Nagel *et al.*, data not shown.
21. We thank D. Stiegert for technical assistance, W. Schwarz for help with pH-sensitive microelectrodes, and D. Gradmann (University of Göttingen) for many helpful suggestions. We are also grateful to U. B. Kaupp (Forschungzentrum Jülich), W. Kühlbrandt (Max-Planck-Institute Frankfurt), B. Ludwig (University of Frankfurt), and W. Stühmer (Max-Planck-Institute Göttingen) for critically reading the manuscript. Supported by the Deutsche Forschungsgemeinschaft (G.N., E.B., and P.H.).

Supporting Online Material
www.sciencemag.org/cgi/content/full/1072068/DC1
Materials and Methods
Fig. S1
References and Notes

20 March 2002; accepted 22 May 2002

A Low Genomic Number of Recessive Lethals in Natural Populations of Bluefin Killifish and Zebrafish

Amy R. McCune,[1]*† Rebecca C. Fuller,[2]*† Allisan A. Aquilina,[1]‡ Robert M. Dawley,[3] James M. Fadool,[2] David Houle,[2] Joseph Travis,[2] Alexey S. Kondrashov[4]

Despite the importance of selection against deleterious mutations in natural populations, reliable estimates of the genomic numbers of mutant alleles in wild populations are scarce. We found that, in wild-caught bluefin killifish *Lucania goodei* (Fundulidae) and wild-caught zebrafish *Danio rerio* (Cyprinidae), the average numbers of recessive lethal alleles per individual are 1.9 (95% confidence limits 1.3 to 2.6) and 1.4 (95% confidence limits 1.0 to 2.0), respectively. These results, together with data on several *Drosophila* species and on *Xenopus laevis*, show that phylogenetically distant animals with different genome sizes and numbers of genes carry similar numbers of lethal mutations.

One of the key genetic processes in any population is the dynamic equilibrium between the mutational origin of deleterious alleles and their eventual elimination by selection. Deleterious alleles maintained by mutation-selection balance create mutation load and contribute to genetic polymorphism and inbreeding depression (*1*, *2*). There are very few estimates of the genomic numbers of even those kinds of deleterious alleles that can individually produce drastic phenotypes and are readily detected by simple genetic assays for lethal and visible recessives. In several *Drosophila* species, the average number of visible alleles per individual ranges from 0.3 to 1.3 (*3*–*5*), and the number of lethals R is 1.0 to 3.0 (*6*–*11*). In *Xenopus laevis*, the only vertebrate for which there are published data, $R \sim 1.9$ (*12*).

Here, we report data on R in natural populations of two phylogenetically distant teleost fishes, *Lucania goodei* and *Danio rerio*. Both *L. goodei* and *D. rerio* were sampled from large wild populations in their native ranges, and a classical design (*3*) was used to detect their recessive alleles. We produced F_1 sibships by individual matings between different wild-caught parents. Within each sibship, individual brother-sister crosses yielded F_2 offspring, which were scored for mutant phenotypes, identified by abnormal morphology. Twenty-five percent of the lethals present in the wild-caught parents will be exposed as homozygotes in offspring from each F_1 cross. When this happens, 25% of the F_2 offspring show the effects of the recessive allele.

For the *L. goodei* experiment, we produced 20 F_1 sibships (*13*) and performed between one and four brother-sister crosses within each sibship. A total of 43 F_1 sib crosses was performed, and 30 to 90 offspring were examined from each cross, resulting in a total of 2569 F_2 offspring, 465 (18%) of which expressed mutant lethal phenotypes. No recessive lethals were found in 17 crosses, and 39 recessive lethals with clear-cut abnormal morphology were observed in the remaining 26 crosses (*14*). The fraction of abnormal F_2 embryos or fry was consistent with a 3:1 Mendelian ratio in all crosses except three, where it was too high. In two of these cases, the proportion of mutant phenotypes was explained better by hypothesizing that two unlinked loci act to produce the same effect. In contrast, only 8 (1.6%) out of 499 F_2 offspring, produced in nine control crosses between F_1 individuals from different sibships, were morphologically abnormal.

Thirty-one different lethals (18 before hatching and 13 after hatching) were found in 20 parental pairs (Table 1). Seventeen prehatching lethals could be subdivided into four clear phenotypic classes. We called them "early death," "worm," "pinhead" (which had several variants), and "bulbous head with beady eyes." They were clearly manifested (*14*) at 1 to 2, 4 to 7, 6 to 9, and 7 to 10 days after fertilization, respectively (Fig. 1). None of these mutants hatched. Twelve lethals that acted after hatching (12 to 14 days after fertilization) could be subdivided into four clear phenotypic classes called "humped," "curly," "uptail," and "no body pigment."

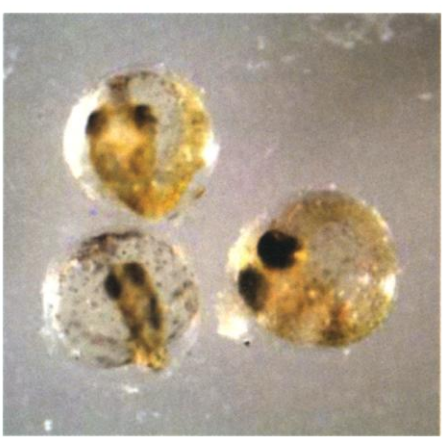

Fig. 1. Mutant and normal phenotypes for *Lucania goodei*. The phenotypes shown were obtained in cross 15b at 8 days after fertilization. The embryo on top is categorized as bulbous head with beady eyes. The embryo on the bottom left is a pinhead with bulbous ventricles. The embryo on the bottom right is wild type.

[1]Department of Ecology and Evolutionary Biology, Cornell University, Ithaca, NY 14853, USA. [2]Department of Biological Sciences, Florida State University, Tallahassee, FL 32306–4340, USA. [3]Department of Biology, Ursinus College, Main Street, Collegeville, PA 19426–1000, USA. [4]National Center for Biotechnology Information, National Institutes of Health, 45 Center Drive, Bethesda, MD 20892–6510, USA.

*To whom correspondence should be addressed. E-mail: arm2@cornell.edu (A.R.M.) and fuller@neuro.fsu.edu (R.C.F.)
†These authors contributed equally to this work.
‡Present address: Department of Biology, Case Western Reserve University, Cleveland, OH 44106, USA.